Microscopic testing of carbon fiber laminates with shape memory epoxy interlayer

Bellisario, Denise; Quadrini, Fabrizio; Iorio, Leandro; Santo, Loredana; Zhang, Zhenxue; Li, Xiaoying; Dong, Hanshan; Semitekolos, Dionisis; Konstantopoulos, Georgios; Charitidis, Costas A.

DOI:
10.1016/j.mtcomm.2022.103854

Materials Today Communications 32 (2022) 103854

Contents lists available at ScienceDirect

Materials Today Communications

journal homepage: www.elsevier.com/locate/mtcomm

Microscopic testing of carbon fiber laminates with shape memory epoxy interlayer

Denise Bellisario [a,*], Fabrizio Quadrini [a], Leandro Iorio [a], Loredana Santo [a], Zhenxue Zhang [b], Xiaoying Li [b], Hanshan Dong [b], Dionisis Semitekolos [c], Georgios Konstantopoulos [c], Costas A. Charitidis [c]

[a] Department of Industrial Engineering, University of Rome 'Tor Vergata', 00133 Rome, Italy
[b] School of Metallurgy and Materials, University of Birmingham, B15 2SQ Birmingham, UK
[c] RNanoLab, School of Chemical Engineering, National Technical University of Athens, Zografos, 157 80 Athens, Greece

ARTICLE INFO

Keywords:
Shape memory polymer composites
Shape memory epoxy foam
Nano-indentation
MicroCT
Thermo-mechanical cycling

ABSTRACT

For the first time, microscopic testing has been performed on shape memory polymer composites (SMPCs) which were manufactured by commercial materials already used in aerospace. Results from micro-tests have been compared with those from conventional memory-recovery cycling on macro-scale. Two shape memory polymer composite (SMPC) laminates were fabricated with different shape memory (SM) interlayer: one in the form of an uncured epoxy powder and the other in the form of a thin epoxy foam. The latter, in particular has been studied to evaluate lightweight and stiff sandwich structures with SM properties. The assessment of the manufacturing process by a hot press moulding technique was assessed through micro scale analysis using SEM and MicroCT analysis. DMA analyses were carried out to understand the interaction mechanisms between raw constituents. A Vickers micro-indentation examination before and after heating was able to assess the shape recovery behaviour at the micro-scale level. A nano-instrumental indentation was used to characterise the shape memory response under different loads at elevated temperatures. Whilst an instrumented thermo-mechanical test allowed to investigate the shape memory behaviour at macro-scale level. Results allow identifying the recovery mechanisms at the micro-scale which are responsible for the shape memory performances at the macro-scale. The higher recovery ability of the SM foam is confirmed in comparison with bulk interlayers.

1. Introduction

Shape memory polymer composites (SMPCs) are smart material structures that can deform in temporary configurations and then recover the initial shape if subjected to specific stimuli (light, heat, magnetic or electric field etc.) [1–4]. In thermally activated structures, the glass transition temperature (T_g) can be used for tailoring the fixing step and the recovery properties of the initial shape [5–7]. Currently, the interest in these smart structures is central in several sectors such as biomedical and aerospace [8–10] where the use of actuators is greatly required [11]. In detail, in the aerospace field, it is fundamental the possibility to use commercial compound materials specifically designed for aerospace. Moreover, the possibility to integrate shape memory properties in commercial materials is an interesting perspective with immediate application impact. The shape memory (SM) behaviour in carbon fibre it is often achieved through the addition of a polymer matrix with SM properties. Really, shape memory polymers (SMP) can be subjected to deformations higher than the ones supported by shape memory alloys (SMA) even if lower actuation load can be exerted upon recovery the equilibrium undeformed configuration [12]. Different polymeric matrix can be selected according to the required functionality. In particular, generally thermosetting resin exhibit better SM properties than thermoplastics, and usually epoxies turn out to have the best performances [13]. In addition, epoxies have also good mechanical and thermal properties and are commonly used in all those manufacturing processes implemented in high impact factories like automotive and aeronautic [14].

The typical techniques to evaluate the shape memory behaviour of the SMP is by applying thermomechanical cycles to quantify the shape memory properties as described by Fulcher [15]. Shape memory

* Corresponding author.
E-mail address: denise.bellisario@uniroma2.it (D. Bellisario).

https://doi.org/10.1016/j.mtcomm.2022.103854
Received 17 January 2022; Received in revised form 4 June 2022; Accepted 13 June 2022
Available online 17 June 2022

polymer has a viscoelastic behavior described through well-established constitutive models also able to predict the main remarkable properties [16] and which is strongly dependent on temperature, therefore it is important to characterize the shape memory response in situ at elevated temperature. Assessing the deformation of the materials on a small scale via Nano-indentation have been well recognized especially at room temperature and recently, some works has been done to examine the thermomechanical and shape recovery behaviour at elevated temperature [17]. The thermomechanical formation and recovery of nanometer-scale indents in a tert-butyl acrylate (tBA)-based shape memory polymer (SMP), was studied by Yang [18] using a heated atomic force microscope (AFM) tip and hot stage atomic force microscopy. However, only the AFM tip was heated and the polymer subjected to indirect heat from the tip during indentation. Fulcher [15] investigated the thermomechanical behavior of a thermosetting shape memory polymer (SMP) by using a high temperature nanoindentation technique. The load–depth curves of the SMP were obtained at various temperatures, from which the instantaneous moduli were calculated with a revised indenter- sample contact depth formula. A large amount of ''sink-in'' is observed at the SMP surface when activated at temperatures above its glass transition temperature (Tg). A framework for understanding the structure (shape memory and thermomechanical) -property relationships in shape memory polymers using indentation is developed by Ming Tian [19].

Shape memory properties can be also evaluated on a macroscale via proper thermomechanical cycles based on tensile (generally for polymers), bending (commonly for composites) or compression (usually for foams) tests and thermomechanical modelling approaches can be further implemented to match experimental data [20]. A systematic approach to investigate thermo-mechanical and shape memory behavior of SMP was proposed by Xu et al. [21]. They performed thermal analysis and shape memory tensile tests on shape memory nanocomposites of polyurethane-clay obtaining that also the addition up to 30%wt if nano-clay do not affect so much shape memory properties. The shape memory behavior of a thermoset-urethane polymer foams with a closed cell structure was investigated by Domeier et al. [22] through compression tests applying different strains up to obtain a 80% foam density with respect to the bulk polymer at different temperatures. Results revealed that higher foam densities exerted recovery stress up to a maximum of 4 MPa. Shape memory polymer foams can be subjected to very high deformation without incurring in damages or failures and can restore almost completely the imposed deformation. Consequently, it is possible to increase the deformation capability of traditional composite laminates by interposing foam cores layer between adjacent plies of carbon fiber reinforced (CFR). This solution allows low density structures characterized by a high percentage of porosity. Latest innovations also include the interposition of functional layers that work as soft cushions for the rigid CFR plies. The functional layers greatly enhance the deformation capability of CFR structures without significantly affects their density. In this regard, a first example was developed by Robinson et al. [23] which interposed polystyrene interleaf layers between CFR laminae. The obtained hybrid composite during transition can be easily shaped in temporary configuration and restore the initial equilibrium shape when re-hated above its transition temperature. This approach allows to use commercial materials during fabrication without major changes or additions compared to the original process.

With this in mind, the authors have already studied SMPC structures using a simple compression molding manufacturing process with commercial materials [24,25]. In particular, aeronautical carbon fiber reinforced prepreg (CFRP) with epoxy matrix and epoxy resin with shape memory properties were used. In this case, the compression molding process allows to cure in a single step the two different epoxy systems, the prepreg matrix of the CFR plies and the SM resin interlayer respectively. Consequently, SMPC structures can be easily developed combining the structural performances of carbon fibers and the SM functionality given by the resin as interlayer [26]. Similarly, this fabrication methodology can be extended to composite sandwich structures with a foam core with SM properties. In particular, the authors developed a solid-state foaming method of an uncured epoxy resin with SM properties [27–30]. In previous works, the authors have studied the manufacturing process of SMPC structures from a macroscopic point of view. In particular, both SMPC structures with thin interlayers [26] and SMPC sandwich with foam cores [31] were studied from the point of view of mechanical behavior and shape memory properties of the structure. In recent works, SMPC structures combining both shape memory epoxy interlayer and SM epoxy foams have been fully investigated [32]. However, the interaction and the SM behavior at the microscopic level of the different layers have never been evaluated. The aim of this study is to fully compare these smart structures both on a micro and on a macro scale, with a particular focus on the resulting meso-structures.

In the light of this, a combination of nano, micro and macro evaluation methods of the SMPC structures was carried out. The aim was observing at the micro-scale the recovery mechanisms which lead to the shape memory behaviour of complex composite architecture. In fact, micro-observations and tests can be carried out on the edge of the laminate by a minimally invasive procedure.

In the experimental procedure, MicroCT scan was used to evaluate the manufacturing process and integrity of the shape memory composites. Vickers micro-indenter was used to pre-indent the polymers followed by heating the polymer to observe the shape restoration initially. A thermomechanical test via nano-instrumental indentation was used to characterize the shape memory response under different loads at elevated temperatures. Optical microscopy (OM) and Scanning electron microscope (SEM) were used to identify and analyse the microstructure changes of the SM at different scales. DMA analyses were also carried out to understand the developed structure coming from the interaction of different epoxy systems obtained by the single step molding process. Furthermore, temperature measurements were performed in order to set the correct configuration and methods for the adopted instrumented thermomechanical tests able to evaluate the SM properties in the macroscale. In this last case, multiple cycles were also developed to analyse the evolution of the shape memory performances. Thanks to this combination of material and structure testing at different scales, the microscopic shape-memory thermo-mechanical behaviour of aeronautical composites is discussed for the first time. In fact, the possibility of producing SM smart devices by using commercial aeronautical prepregs, and state-of-the-art moulding technologies, was already shown [26,32] but the discussion of related micro-mechanisms has never been made yet.

2. Materials and methods

2.1. Raw materials and manufacturing

The shape memory polymer composite (SMPC) structures consist of two prepreg layers with the interposition of one SMP interlayer. Commercial thermosetting CFRP prepregs (HexPly M49/42%/200PW/CCF-3 K) supplied by Hexcel and commercial epoxy uncured powder (3 M Scotchkote 206 N) were used. In particular, the epoxy resin was used in two different forms: as is and as foam after solid state foaming process already reported in previous work of authors [22]. The epoxy foam was used as central thin layer of 1.2 ± 0.02 mm of thickness with a density of 0.41 g/cm^3 between two ply of CFRP to form a sandwich structure (Fig. 1a). The epoxy resin was also interposed as is in a layer of 0.1 mm between two prepreg laminae (Fig. 1a). The second type of SMPC structure was produced interposing the thin epoxy foam slice between two layers of prepreg. A compression molding process over a hot plate at 200 °C for 60 min under an applied pressure of 66.7 kPa through an aluminium mold was used to produce samples with 50x10mm^2 and 100x30mm^2 nominal dimensions for thermal analysis and shape memory behavior tests respectively, as shown in Fig. 1b.

Moreover, microscopic observation and characterization were

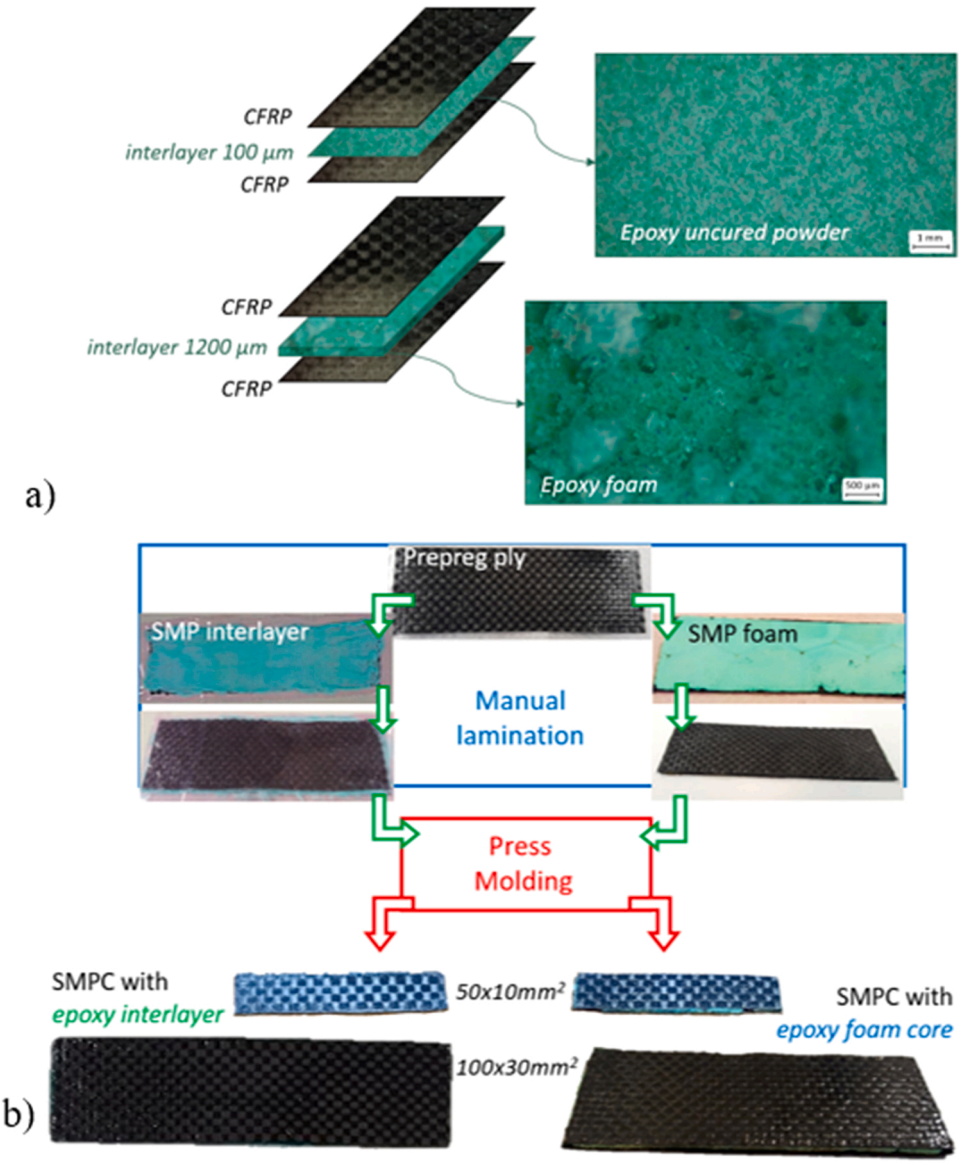

Fig. 1. a) Schematic of SMPC structures and b) procedure for SMPC samples manufacturing.

carried out on samples of 5×10 mm^2 cut from molded samples with one resin interlayer, with 4 resin interlayers and with a thin foam core. After molding, sample thickness was measured, and it was 0.43 ± 0.20 mm and 1.40 ± 0.02 mm for the bulk and foam interlayer, respectively. The high dispersion of thickness for the thinner laminate was due to the adopted laboratory procedure, and was mainly dependent on the presence of epoxy resin on the sample edges. Previous studies have shown that this variability reduces by increasing the number of composite plies [24,25]: 4-ply laminates have an average thickness of 1.67 ± 0.01 mm. It was observed that shape memory properties of 2-ply laminates can change from one sample to another because of this variability. However, the effect of the number of plies is stronger than the thickness uniformity.

2.2. Scanning electron microscope and optical observations

A JEOL 7000 FE Scanning Electron Microscope (SEM) equipped with EDX was used to reveal the reliability of the manufacturing process used to fabricate the different SMPC structures.

Micro computed X-ray tomography is a powerful tool to monitor both the manufacturing weaknesses and the failure mechanisms of composites. A Nikon XT H225 with processing software of VolumeGraphics was used to scan the composite samples to carry out the 3-D characterization of the composite samples. The versatile XT H 225 systems offer a microfocus 225 kV microfocus X-ray source with 3 μm focal spot size.

2.3. Micro-mechanical characterization

The micro Vickers hardness tests were performed by Mitutoyo MVK-H1 micro-hardness machine on SM interlayer. In particular, for the type of test, only continuous interlayer was analysed and not the shape memory foam. A standard Vickers micro-hardness indenter was used to micro-indent the SMP interlayer in order to evaluate the shape memory properties of the material at a micro scale. The Vickers hardness test with a Vickers diamond indenter, that is a right pyramid with a square base and an angle of 136° between opposite faces. The two diagonals of the indentation left in the surface of the material after removal of the load which have various depth depending on the load. The shape memory samples were cut into thin slices of 1–2 mm thick and stuck on a metal plate with ceramic slurry, once dried and they were ground and polished for micro-indentation test. A series of indentations were made

under various loads (10, 25, 50, 100 and 200 g), and after put into a furnace at 190 °C for 10 min, and then again observed to evaluate the recovery of the deformed area.

A NanoTest system produced by Micro Materials Ltd., Wrexham, UK was used for the nanoindentation testing. The system has a very high thermal stability enabling nanoindentation creep measurements to be performed without thermal drift. A heating block was attached to the sample holder to heat the sample. The temperature was controlled using a K-type thermocouple embedded in the hot stage of the instrument. The samples were heated up at a rate of 1.6 °C/min to the target temperature i.e. 100 °C and stabilise for about 30 min and it was kept constant throughout the test. The initial (contact) load was 10 μN. All the samples were loaded from this initial load to a peak load at a specified loading rate, i.e. 1 mN/s. Loads up to 500 mN have been applied. Different loads from 10 mN up to 500 mN were applied in a loading rate of 1mN/S on the shape memory polymer matrix for 5 s to investigate the micro-mechanical properties. The test was normally carried out three times under same conditions at room temperature, and elevated temperature like 80 °C, 100 °C and 110 °C. An in-site optical microscope was used to select the test zone and observer the indentations. This kind of test has been used for the first time in this study for evaluating the SM behaviour of theepoxy interlayer of the composite laminate. Testing parameters have been set to monitor the different material behaviour as a function of the temperature but some issues are present. Mainly, a difference in temperature between the tip and the sample is expected as well as a possible non uniform temperature distribution in the sample [10]. For this reason, other tests on a bigger scale (such as DMA shape recovery tests) have been performed for comparison. Temperature uniformity during shape recovery is not possible, as the material changes the shape during the time this uniformity is reached. For this reason, it is always difficult to give a temperature reference for the shape trigger, and processing temperatures are preferred for this aim.

2.4. Macro evaluations: thermo-mechanical analysis and shape memory performances

Dynamic mechanical analysis (DMA) was carried out to evaluate the interaction between different epoxy systems, as the prepreg matrix of the SMP interlayer and the SM epoxy resin/foam respectively. Instead, the thermal analysis of the SM epoxy resin in the different forms was previously carried out in other studies. In particular, the differential scanning calorimetry (DSC) analysis of the uncured epoxy powder [28] and of the epoxy foam [28,33] were performed and reported in previous works of authors. In the current study, DMA tests (by Netzsch DMA242C) have been performed on the two smart composite structures with interlayer and with foam core in a three-point bending configuration. The temperature scans were carried out from room temperature (T_{room}) to 200 °C at 5 °C/min with the frequency of 10 Hz and the span-length of 40 mm.

A series of shape memory tests at the macro scale were performed in order to demonstrate the SM performances on the fabricated samples used in the current experimentation. The experimental procedure for SMPC memory-recovery cycles has been discussed in several previous studies [24–26]. Both the bending configuration and the heating procedure are optimized to maximize the functional behavior of SMPCs in conditions close to possible applications. The main constraints are the need of fast heating and cooling as well as the need of high sample displacements during shape change. Shape evolution of the SMPC occurs in the transient state of the material, and it is not possible to assume a uniform material temperature during this stage. Nevertheless standardization is necessary for comparison of different samples.

The SM tests were carried out with a universal testing machine (MTS Insight 5) equipped with a cantilever system to maximize sample's inflection, in order to perform cyclic tests consisting of: sample deformation, fixing of the temporary shape (memorization) and restore of the initial one. This kind of test is commonly referred as "thermo-mechanical cycle". At T_{room} a load is applied to the sample up to the maximum inflection deformation at 1 mm/min of test speed and with a free inflection length of 80 mm. The inflection is maintained for a fixed time during which samples are first heated with a hot air gun positioned at 30 mm from the sample surface over glass transition temperature (T_g) and then are left to cool down T_{room} (Fig. 2a). After, the thermo-mechanical cycle is finally closed by restoring the initial undeformed shape upon heating sample up to a recovery temperature Tr = Tg+ 20 °C. The shape memory behavior in terms of shape fixity (Rf) and shape recovery (Rr) was quantified by means of the equations reported by Quadrini et al. [26]. Temperature monitoring during thermo-mechanical cycle was carried out with a k-type thermocouple and recorded with a dedicated SW by OMEGA. A single thermocouple has been placed on the surface opposite to the heating flux in order to check the temperature during test. Several consecutive thermo-mechanical tests have been performed for each SMPC structure. In particular, a first three-cycles test was performed increasing the maximum strain for each cycle (0.06%, 0.12% and 0.18%) for each SMPC structure (Fig. 2b). The maximum imposed deformation is a trade-off value among technical limits of the cantilever adjustable system which has been set considering the SMPC specimen with epoxy interlayer as reference specimen being suitable for larger inflections. Finally, 5 consecutive instrumented thermomechanical cycles were carried out at the maximum imposed strain of 0.18% (Fig. 2**c**) and the shape memory performances at the end of the multiple test were evaluated. In this case, a test speed of 2 mm/min was set to optimize the overall testing time. At the end of the multiple cycling, no damages were observed on samples.

3. Results

3.1. Evaluation of the composite structure

The SMPC structures after fabrication were measured and the average thickness of the sample with resin interlayer was 0.47 mm and with thin foam layer of 1.46 mm. As expected, the two developed smart structures show different density values:1.39 g/cm^3 and 0.82 g/cm^3 for the SMPC with epoxy interlayer and with epoxy foam thin layer respectively on average. The layered structures are shown by the optical images in Fig. 3 obtained through a Leica S9i stereoscope for both SMPC structures.

SEM images show the two developed SMPC structures and clearly identify the stacking sequence between CFR ply and shape memory interlayer as well as the good bonding between them (Fig. 4a-b).

Carbon fiber/polymer interface with SMP interlayer reveal very good adhesion between CFR ply and shape memory interlayer. Similar good results were also obtained in the case of a multi-ply SMPC laminate with five CFRP ply and four SMP interlayers (Fig. 4c). A compact structure is visible and the increase of number of plies has not resulted negatively to the laminate integrity and homogeneity. In Fig. 4d and Fig. 4e is depicted uniformly distributed pores of SMP foam between two CFR laminae. The SMPC structure with foam as interlayer also underlined a good bonding with the CFRP plies.

The cross-sectional image of the CFRP with SMP interlayer can be seen in the optical microscopy image on Fig. 5a, and the layer by layer structure can be examined by Micro-CT scan Fig. 5b. 3D inspection of the composite can reveal how the thin shape polymer interlayer is well connected with the plies of the CF fabric and reveal the distribution and geometrical properties of the composite, pores and other inhomogeneities. The shape memory polymer interlayer has interacted well with the Carbon Fibre laminates. MicroCT scan of the SMPC with epoxy foam underline as the foam layer is much thick than the two plies and there is a large amount of the pores in the foam which is expected from the type of material (Fig. 5d-e). Moreover, SEM observations clearly shown the pores and the good connection among foam and the carbon fiber fabric plies (Fig. 4d-e).

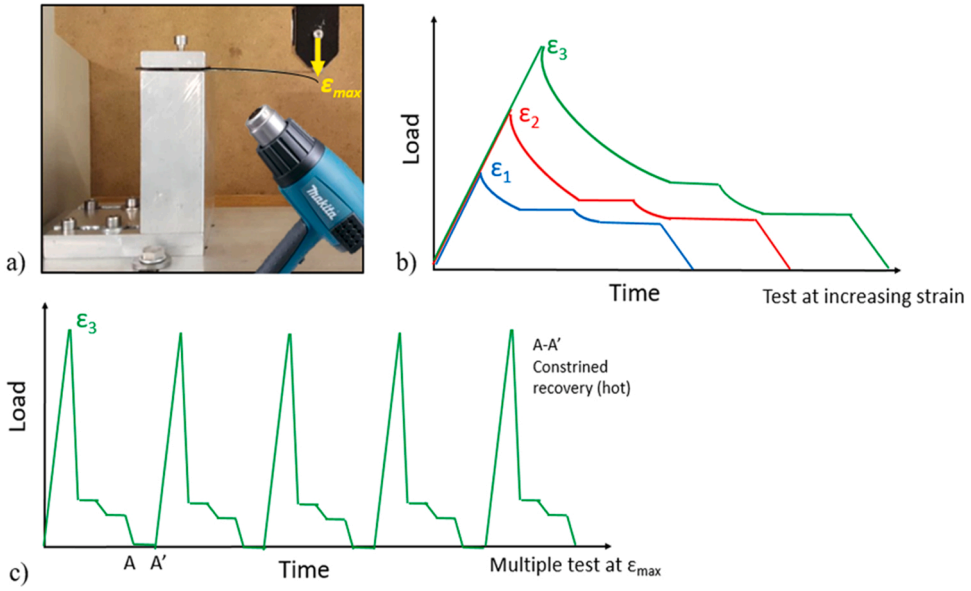

Fig. 2. Shape memory tests: a) Test setup; b) increasing maximum strain; c) multiple consecutive thermo-mechanical cycles.

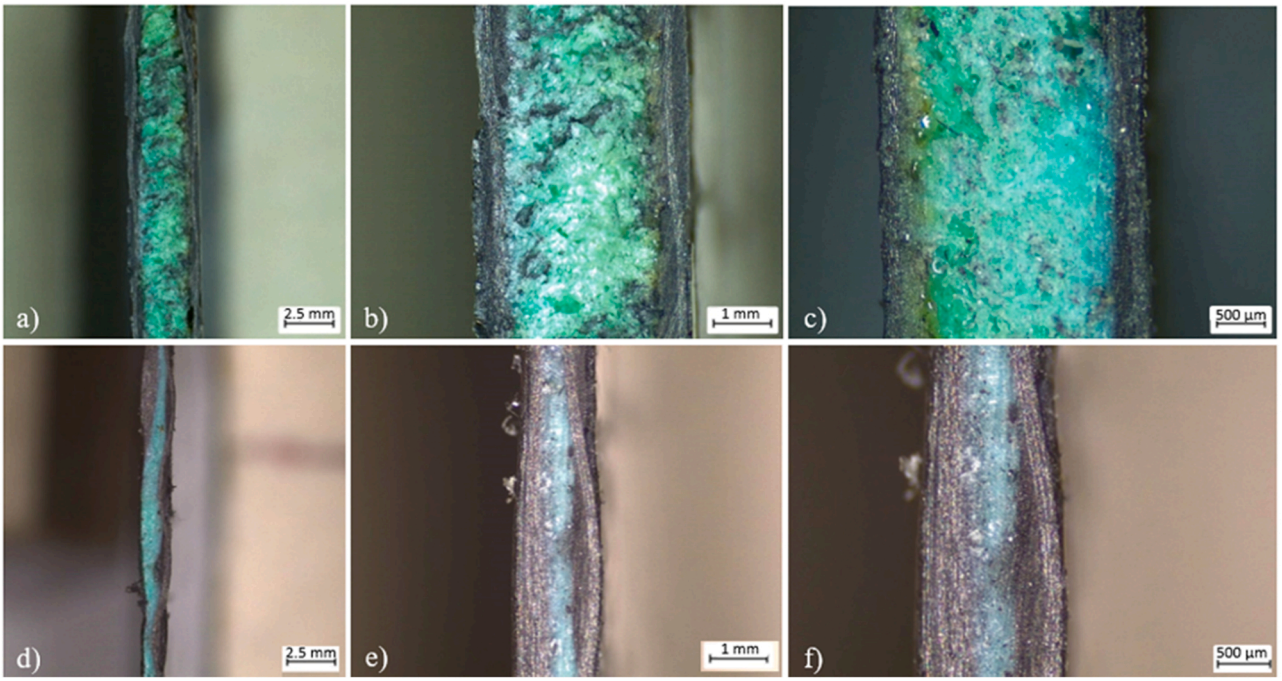

Fig. 3. Cross sectional optical images of SMPC with epoxy foam layer (a-c) and with epoxy interlayer (d-f).

Micro-CT arithmetical analysis of the samples allowed to assess the distribution and geometrical properties of the functional additions, pores and other inhomogeneities. The 3D Images from CTVox software are shown in Fig. 5c and Fig. 5f. The pores are highlighted with dark red colour and it is confirmed that the CFRP exhibits a small amount of porosity (0.45%). It can be also seen that the shape memory polymer interlayer has interfered with the Carbon Fibre laminates. As observed in SEM images, the shape polymer interlayer appears to have created a uniform layer between the plies of the CF fabric. However, it can be also observed that the epoxy foam shape memory polymer creates a wide amount of porosity inside the material (17.21%), something that is expected to happen since a foam intertwines between the CF fabric plies.

DMA is a generally used technique to examine the viscoelastic properties of flexible polymers and polymer foams. In Fig. 6a and b storage modulus (E') and tan δ are plotted as a function of temperature for the two different SMPC structures.

The DMA analysis showed that the storage modulus of SMPC with epoxy interlayer is always higher on the whole temperature range, from 32% to over 90% whereas loss factor is lower in the transition zone where the peak is nearly 2.5 times lower. This occurrence is related to the different state of the two interlayers and in particular to the higher damping properties of foam. In terms of T_g, the SMPC with epoxy interlayer has a value of 118.7 °C (considering the inflection point of E') which reduces to 107.5 °C for the SMPC with epoxy foam. The same difference could be observed analysing the T_g extracted with the tanδ peak, and in particular, the SMPC with epoxy interlayer highlighted a T_g of 123.6 °C and the SMPC with epoxy foam reduced to 117.3 °C. The transition onset is anticipated of about 25 °C for the SMPC with epoxy

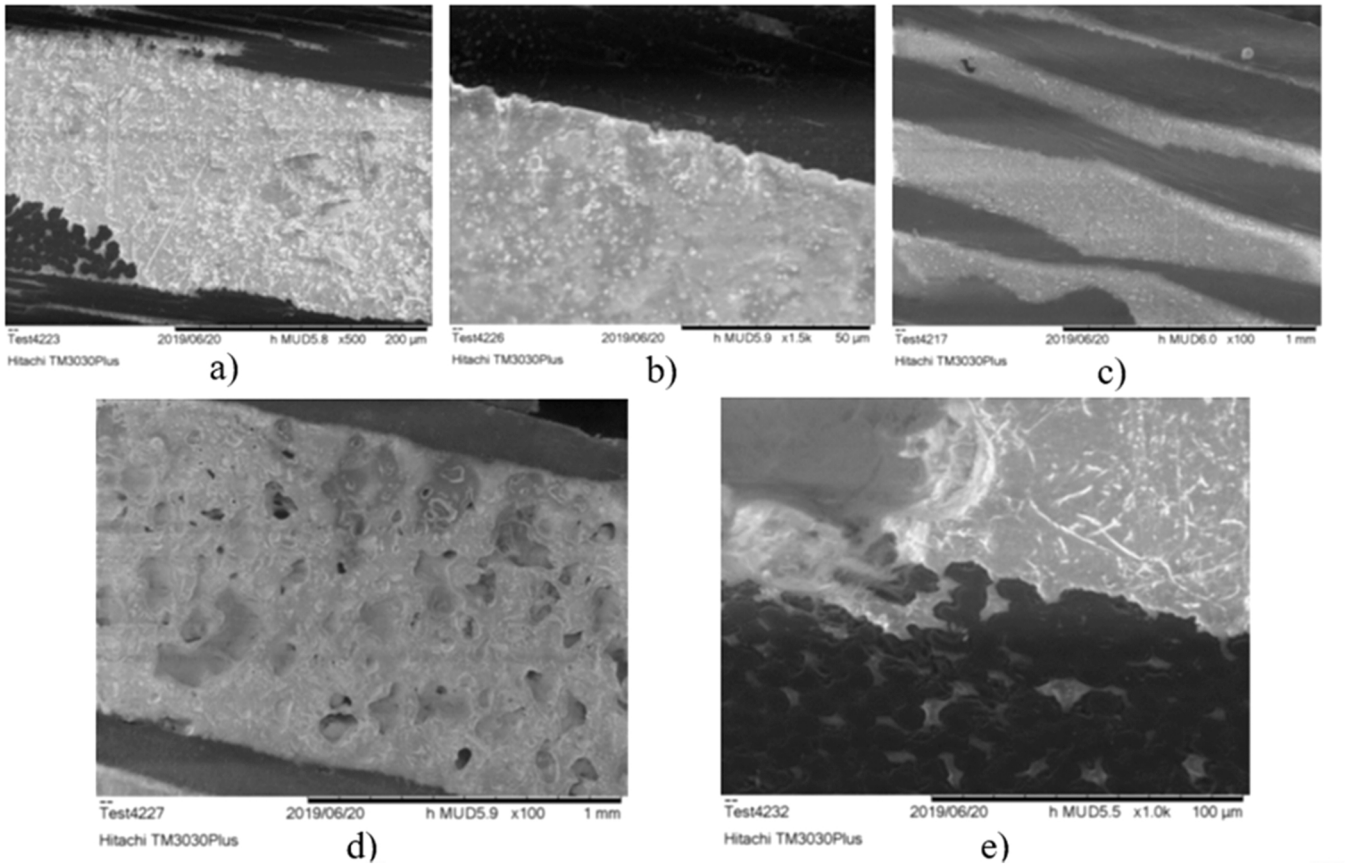

Fig. 4. SEM analysis of the cross section of SMPCs (a,b) with single epoxy powder interlayer, (c) with 4 epoxy powder interlayers and (d,e) with epoxy foam thin layer.

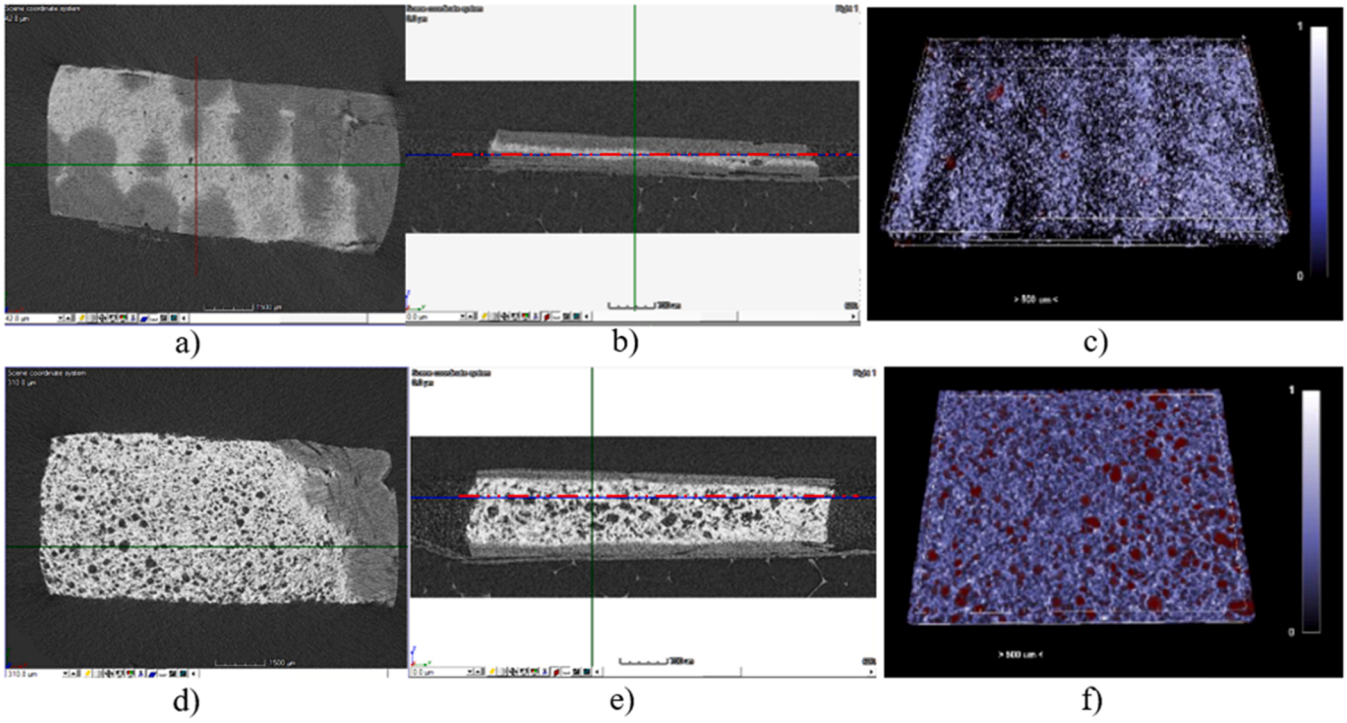

Fig. 5. Micro-CT scan and analysis of the SMPCs a) cross sectional, b) side view and c) analysis of SMPC with epoxy powder interlayer and d) cross sectional, e) side view and f) analysis of SMPC with epoxy foam thin layer.

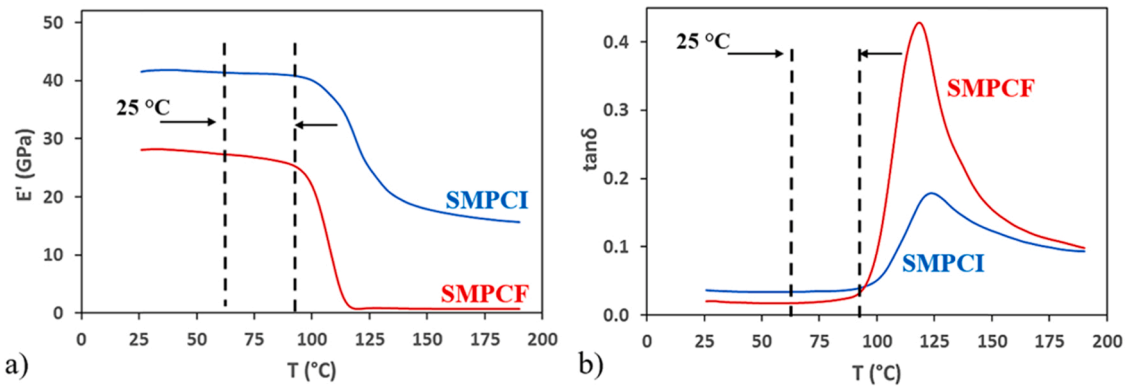

Fig. 6. Storage modulus E' a) and loss factor b) from DMA tests on SMPC with epoxy interlayer (SMPCI) and with epoxy foam thin layer (SMPCF).

foam layer whereas the transition range is narrower being of about 25 °C (considering E' curve) against almost 40 °C for the SMPC with epoxy interlayer. Differences may be expected due to the final forms of the SM epoxy resin, interlayer and foam, and not by the nature of the raw constituents being the same.

3.2. *Mechanical response of the shape memory composite at micro, nano and macro level*

Vickers micro-hardness indentations have been observed before and after heating for assessing the response temperature of the shape memory effect. The indentations (50 g/25 g/10 g) on the shape memory layer can be seen before heating (Fig. 7a) and the 25 g and 10 g indentations disappeared after heating due to the shape recovery, meanwhile, indentation under 50 g has restored most of its shape with a slightest trace (Fig. 7b) which is an indication of the shape memory response. However, the indentations on the prepreg layer remained intact after heating cycles (Fig. 7c).

Nano indentation was used for the in-situ response of shape memory behaviour of SMP interlayer and foam. Indentations at different loads of 50/100/400 mN have been impressed at room temperature (RT) before the test at elevated temperatures to check the change of the impression after heating/cooling process. In particular, the testing temperatures were made to vary in step of 10 °C between 80 and 90 °C and 110–130 °C to observe the changes around the T_g of the SMP. The maximum temperatures set are those relating to the detection of a decrease in the displacement under load at the same load. For the shape memory interlayer, the displacement verse load (max 50 mN) relationship at the different temperatures are shown in Fig. 8 and the corresponding nano-hardness and reduced elastic modulus are compared in Table 1. Only one test was performed for each nano-indentation condition because of the experimental difficulties. Repeatability was

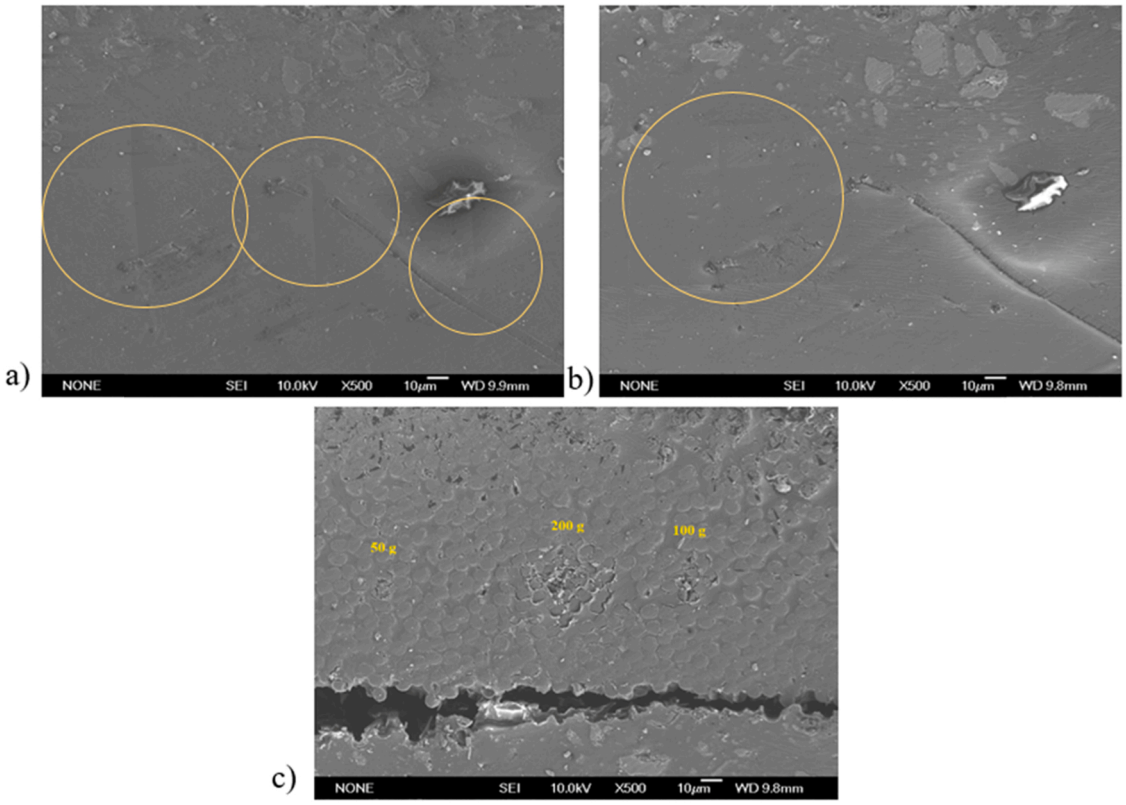

Fig. 7. Three indentations (50/25/10 g) on the shape memory layer before (a) and after (b) heating at 190 °C for 10 min, (c) The indentations on the prepreg layer after heating.

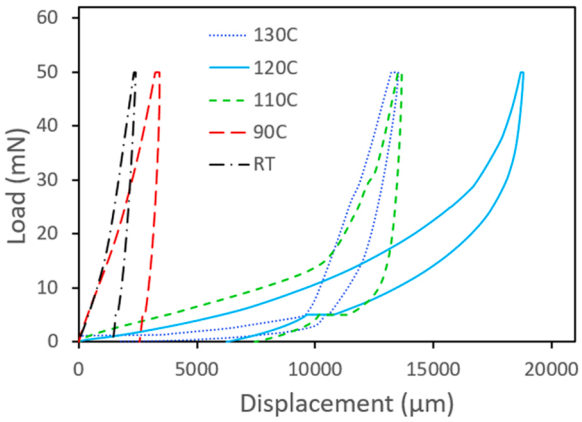

Fig. 8. Response of shape memory epoxy interlayer at different temperatures under a load of 50mN.

Table 1
Nanohardness and reduced elastic modulus of the shape memory interlayer at different temperatures.

Temperature (°C)	Hardness (GPa)	Er (GPa)
RT	0.632	10.14
90	0.206	6.79
110	0.013	0.89
120	0.008	0.10
130	0.013	0.41

checked initially at room temperature, and was considered in the expected variability range.

When operated at higher temperatures, the SMP exhibits surface profiles different from those obtained when carried out at room temperature as reported by Fulcher et al. [15]. The increase of displacement was slower at temperature lower than 100 °C and it became much deeper and distorted when temperature was higher than 100 °C and reached the highest value at 120 °C. The displacement increased with the temperature and it might be due to the shape memory layer which became softer at elevated temperature. However, the displacement decrease for the test at 130 °C which suggest the response of the shape memory effect led to the shape recovery. Further check on the indentations pressed at room temperature indicated that they can still be discernible after being heated up to 110 °C, and they became lighter and smaller after heating at 120 °C while it disappeared totally at temperature above 130 °C. Therefore, the triggering temperature for this SMP interlayer is between 120 and 130 °C, as also confirmed by previous DMA analysis.

Similarly, for the shape memory foam, the indentation depth increased with the temperature as seen in the displacement verse load curve and the SEM image of indentations at 80 °C and 100 °C (Fig. 9a, b) which might be due to the soft effect of the shape memory layer with elevating temperature. However, the depth of the indentation reduced at 110 °C (Fig. 9a). The indentation depth on shape memory foam composite increased with the load at room temperature, and the impressions remained after heating till 100 °C as seen in Fig. 10. The indentations were fully recovered after heating to 110 °C due to the shape memory effect. The temperature required for complete recovery of the indents is between 100 and 110 °C which the SM effect can be triggered for the shape memory epoxy foam in the composite, as also confirmed by previous DMA analysis.

The results of the thermomechanical cycle on the SMPC structures attested also the SM properties in the macro-scale for the two different SMPC structures. During the heating and cooling cycle, the temperature was monitored to assess the achievement of the T_g for the SMPC structure. Temperature acquisition started when maximum inflection was reached. In the complete thermomechanical cycle, two heating steps are present: one related to the memory step and the other related to the recovery step. For the SMPC with epoxy powder interlayer, average values of 130 °C and 120 °C were recorded for the first and the second heating respectively. Similarly, for SMPC structure with thin epoxy foam layer, the average values were 124 °C and 112 °C were recorded. Temperature monitoring showed that 120 s are sufficient to guarantee a uniform heating and cooling on the whole structures.

In Table 2 the shape fixity (R_f) and shape recovery (R_r) values for the three imposed maximum strains and after a 5 cycles test at the highest maximum strain were summarized for both of the two SMPC structures.

When increasing the maximum imposed deformation, the CFRP with SMP interlayer exhibits an increase in the R_r and a decrease in the R_f. The effects of multiple cycles are clearly evident in SMPC with epoxy interlayer where the R_r reduces down to 70, whereas R_f increases up to 77% as result of the residual deformation of previous cycles not fully recovered. In the case of SMPC with epoxy foam layer opposite trends are instead exhibited, that is, the increase of R_f and the reduction of R_r when increasing the level of strain. These trends were confirmed also after multiple thermomechanical cycles.

4. Discussions

High performing SMPC structures must necessary combine mechanical performances and optimal functionalities given by the carbon fibres and the resin matrix respectively [30,31]. Typically, each raw constituent exalts its own properties negatively affecting the other ones when considered in the final structures; for this reason, it is crucial

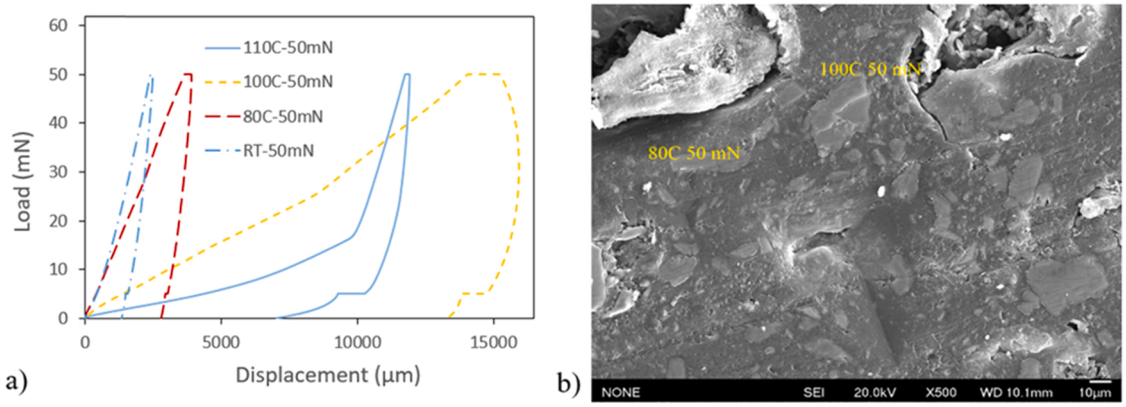

Fig. 9. (a) Response of shape memory foam (S5) at different temperature under a load of 50 mN, and (b) the indentations produced at 100 °C and the indentation produced when the temperature reduced to 80 °C.

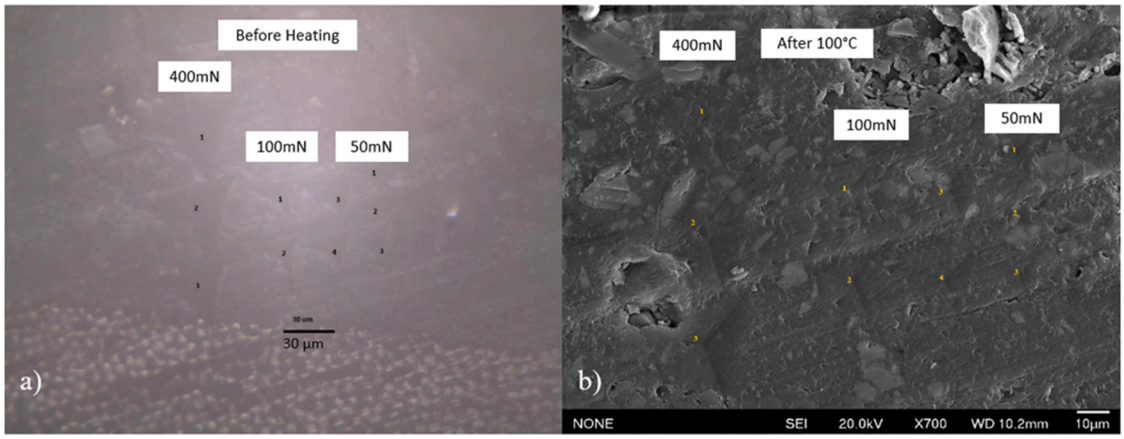

Fig. 10. The change of the indentations on the shape memory foam under different loads (a) at room temperature, and (b) after heating to 100 °C.

Table 2
Shape memory properties of the manufactured SMPC structures at increasing strains and after multiple consecutive thermos-mechanical tests at maximum set strain.

	SMPC with epoxy interlayer				SMPC with epoxy foam thin layer			
	ε_1 (%)	ε_2 (%)	ε_3 (%)	5 cycles at ε_3 (%)	ε_1 (%)	ε_2 (%)	ε_3 (%)	5 cycles at ε_3 (%)
	0.06	*0.12*	*0.18*	*0.18*	*0.06*	*0.12*	*0.18*	*0.18*
R_f (%)	71.3	64.2	49.6	76.8	54.9	73.6	82.1	86.5
R_r (%)	95.4	95.8	99.4	69.5	100	98.7	96.1	87.8

determine an optimal compromise which allows to maximise as much as possible the different required contributions. In this optic, manufacturing technologies help to pursue these objectives finding the suitable solutions for each required application. The two developed SMPC structures obtained starting from commercially available materials, an aeronautical prepreg and an uncured SM epoxy resin, were produced using a compression molding process. As SM interlayer between CFR plies were interposed two different form of the same epoxy resin as uncured resin and as foam in order to fabricate two different SMPC structures. The layered structures are clearly shown in optical images of Fig. 4. In both cases good adhesion was obtained between CFR plies and interlayers as revealed by SEM images in Fig. 5. These observations assess the soundness and the reliability of the adopted manufacturing procedure. In the used compression molding process, the resin bleeding of the prepreg matrix is able to establish optimal interaction with both types of interlayers. Specifically, the interaction of the prepreg resin with the SM resin of the interlayers lead to new meso-structures, due to the two different epoxy systems. Different mechanisms take place depending on the physical state in which the SM interlayer occurs. In particular, for the epoxy powder interlayer, resin bleeding affects all discontinuities among powder whereas in case of the epoxy foam layer, resin fills all voids resulting from the closed-cell structure of the foam itself. SEM images also show the interlayer thickness homogeneity of laminates. These results prove the ability of the manufacturing process used to fabricate these SMPC structures. A quantitative analysis was achieved through MicroCT which revealed the porosity level of both SMPC structures. As expected, foam is responsible of the higher content of void, being 38 times higher than its interlayer counterpart. This result is reasonable if considering that foam is nearly ten times thicker than the epoxy powder interlayer so increasing the development of porosity on the whole foam structure itself. Macroscopically it is reflected in the lower density value which reduces of 41%.

The thermo-mechanical behaviour of the SMPC fabricated structures were assessed by DMA analysis. The existence of a single transition zone for both SMPCs confirms that a unique meso-structure was developed in both cases despite the presence of two different epoxy systems. Glass transition temperature results lower for the SMPC with epoxy foam. This emphasizes how the epoxy foam activates the molecular mobility sooner than the epoxy uncured interlayer. The difference in the thermo-mechanical analysis could also be due to the higher amount of the SM resin present in the thicker foam. This also interferes with the transition onset being anticipated of about 25 °C with respect to the SMPC with epoxy powder interlayer. This occurrence speed-up the recovery process but limits the application in those fields where a rigid structure is required also in that range of temperature. At last the transition zone is narrower when epoxy foam as interlayer is used and this is a remarkable property for SM materials because this characteristic guarantees a trigger effect upon recovery. With this in mind, for the production of smart structures, the optimal solution must be tailored for the specific range of use.

Nano indentation tests revealed the shape memory behaviour locally and at micro scale. It was observed that for the maximum applied load of 50mN the maximum penetration depth was obtained for a temperature of about 120 °C and 100 °C for the epoxy powder interlayer and for the epoxy foam respectively. These temperatures values are in agreement with the T_g results obtained via DMA, especially for the SMPC with epoxy powder interlayer. In fact, about 2 °C of variation on average are exhibited with respect to the minimum value of T_g related to the inflection point of E' (118.7 °C) and to the maximum value related to the peak of tanδ (123.6 °C). Higher discrepancies were instead observed in the case of SMPC with epoxy foam where the closest value was the T_g value related to the inflection point of E' (107.5 °C). This discrepancy can be dependent to some structural inhomogeneities easily developing in the epoxy foam rather than in the thinner epoxy powder interlayer. Furthermore, nano-indentation reached higher values for the epoxy powder interlayer up to 19×10^3 µm verse nearly 15×10^3 µm obtained for the epoxy foam, with an increase of 27%.

Instrumented thermomechanical cycle allowed to complete the SM behaviour characterization also at a macroscale. The temperature to activate molecular mobility was set accordingly to the results of DMA and nano indentation, in particular a transition temperature $T_t = T_g + 20$ °C was chosen due to the distance of about 30 mm of the thermal source. This distance was chosen because shorter distances led

to degradation of the CFR matrix and the MS polymer. Shape fixity for SMPC with epoxy powder interlayer is limited by the elastic contribution of the carbon fibers which is typical for laminate with few ply and even more evident when increasing the maximum imposed deformation. Otherwise, the SMPC with SMP foam showed the opposite behaviour due to the intrinsic properties of the two different structures. In particular, foams tend to cause cells collapse under a large imposed deformation overturning the possibility to gain high shape recovery values, but allowing a greater ability to fix the shape without damaging the external ply. Specifically, the highest values of R_f and R_r are recorded for SMPC with SMP foam which reaches also 100% of R_r for the lowest deformation applied. At the end of the multiple cycling, R_f of the SMPC with epoxy interlayer exhibit a maximum of 77% which can be attributed to the small and progressive amount of residual deformation at each cycle. This behavior is intrinsic to the type of structure of the interlayer and to the higher stiffness at room temperature of the structure. On the opposite, the SMPC with epoxy foam interlayer still exhibits notable shape memory performances. The two structures have different areas of use and even the differences highlighted can be enhanced depending on the use. In particular, the SMPC structure with epoxy interlayer can maximize shape memory properties by increasing the number of layers and interlayers as reported in previous works [26].

5. Conclusions

In this study two different SMPC structures suitable for aerospace use were produced by compression molding of commercially available materials. For the first time, a long carbon fiber laminate from commercial thermosetting aeronautical prepregs is tested for its microscopic shape memory behaviour. The role of the SM interlayer is discussed on microscale as a function of its structure. Proposed composite laminates combined structural performances of carbon laminates with the functionality of shape memory polymers. In particular, the two SMPC structures differ in the SM layer interposed: one had a thin layer of SM epoxy resin, and the other had a SM epoxy foam. The two structures were manufactured in order to evaluate the applicability of an aeronautical molding process, such as compression molding, in the manufacture of smart structures for aerospace. That is an important achievement of the study as most of proposed innovative SMPC materials from the scientific literature cannot be considered as aeronautical materials.

SEM and MicroCT images confirmed a good adhesion between CFRP ply and epoxy interlayer either as thin film or as thin foam layer. SEM images highlighted the uniformity of the thin SMP interlayer obtained during composite lamination, with a very low percentage of porosity in CFRP ply as revealed by MicroCT analysis. DMA investigations showed an effect of SM interlayers on the transition zone which becomes narrower when larger amount of SM resin is used. The shape recovery behaviour was assessed at micro and nano level by means of microindentations and nano-instrumented indentations. In particular, the nano-instrumented technique was used for the first time on this class of SMPCs, and allowed calculating the shape memory response temperature at a narrow range for both SMPC structures. Finally, the shape memory behaviour of SMPC structures has been validated through thermo-mechanical cycles with increasing strain and multiple thermo-mechanical cycles at the macroscopic level. Higher SM performances are exhibited by the SMPC with the thin epoxy foam layer as expected due to the foam structure. On the opposite, SMPC with epoxy powder interlayer shows lower but remarkable SM properties. The multiple thermo-mechanical cycling affects the SM behaviour without compromising the structural integrity of the developed smart structures. Moreover, an accurate design of the type and number of SM epoxy interlayer could significantly improve the shape memory performances.

CRediT authorship contribution statement

For research articles with several authors, a short paragraph specifying their individual contributions must be provided. Conceptualization, Denise Bellisario and Fabrizio Quadrini; Methodology: Xiaoying Li, Hanshan Dong and Dionisis Semitekolos; Investigation: Leandro Iorio and Georgios Konstantopoulos; Data curation, Zhenxue Zhang and Leandro Iorio; Formal analysis, Denise Bellisario; Resources: Fabrizio Quadrini and Costas A. Charitidis; Resources, Loredana Santo; Validation, Fabrizio Quadrini and Zhenxue Zhang; Writing – original draft, Denise Bellisario; Writing – review & editing, Fabrizio Qudrini and Zhenxue Zhang. All authors have read and agreed to the pub-lished version of the manuscript."

Funding

This research was supported by the European Union's Horizon2020 research and innovation programme under Grant Agreement n. 760779 named 'Smart by Design and Intelligent by Architecture for turbine blade fan and structural components systems' (SMARTFAN).

Declaration of Competing Interest

The authors declare no conflict of interest. The funders had no role in the design of the study; in the collection, analyses, or interpretation of data; in the writing of the manuscript, or in the decision to publish the results.

References

[1] H. Lu, S. Du, Polym. Chem. 5 (2014) 1155–1162.
[2] H. Lu, F. Liang, J. Gou, Soft Matter 16 (2011) 7416–7423.
[3] Y.M. Razzaq, M. Behl, M. Heuchel, A. Lendlein, Macromol. Rapid Commun. (41) (2020) art.no. 1900440.
[4] J.M. Robertson, A.H. Torbati, E.D. Rodriguez, Y. Mao, R.M. Baker, H.J. Qi, P. T. Mather, Soft Matter 11 (2015) 5754–5764.
[5] J. Meng, J. Hu, Compos. Part A 40 (2009) 1661–1672.
[6] A. Basit, G. L'Hostis, B. Durand, Mater. Lett. 74 (2012) 220–222.
[7] M. Herath, J. Epaarachchi, M. Islam, L. Fang, J. Leng, Eur. Polym. J. 136 (2020).
[8] F. Li, L. Liu, L. Du, Y. Liu, J. Leng, Compos. Struct. 242 (2020).
[9] Y. Liu, H. Du, L. Liu, J. Leng, Smart Mater. Struct. 23 (2) (2014).
[10] M. Lei, Z. Chen, H. Lu, K. Yu, "Recent progress in shape memory polymer composites: methods, properties, applications and prospects, Nanotechnol. Rev. 8 (2019) 327–351, https://doi.org/10.1515/ntrev-2019-0031.
[11] M. Sobczyk, S. Wiesenhu, J.R. Noennig, T. Wallmersperger, Smart materials in architecture for actuator and sensor applications: a review, J. Intell. Mater. Syst. Struct. (2021), https://doi.org/10.1177/1045389X211027954.
[12] I. Stachiv, E. Alarcon, M. Lamac, Shape memory alloys and polymers for MEMS/NEMS applications: review on recent findings and challenges in design, preparation, and characterization, Metals 11 (2021) 415, https:// doi.org/10.3390/met11030415.
[13] J. Karger-Kocsis, S. Kéki, Review of progress in shape memory epoxies and their composites, Polymers 10 (2017) 34, https://doi.org/10.3390/polym10010034).
[14] M.G. Wimmer, B.G. Compton, Addit. Manuf. 54 (2022) art.no. 102725.
[15] J.T. Fulcher, Y.C. Lu, G.P. Tandon, D.C. Foster, Thermomechanical characterization of shape memory polymers using high temperature nanoindentation, Polym. Test. 29 (5) (2010) 544–552.
[16] X. Xin, L. Liu, Y. Liu, J. Leng, Mechanical models, structures, and applications of shape-memory polymers and their composites, Acta Mech. Solid. Sin. 32 (5) (2019) 535–565, https://doi.org/10.1007/s10338-019-00103-9.
[17] E. Wornyo, K. Gall, F. Yang, W. King, Nanoindentation of shape memory polymer networks, Polymer 48 (11) (2007) 3213–3225.
[18] F. Yang, E. Wornyo, K. Gall, W.P. King, Thermomechanical formation and recovery of nanoindents in a shape memory polymer studied using a heated tip, Scanning 30 (2) (2008) 197–202.
[19] M. Tian, T.A. Venkatesh, Indentation of shape memory polymers: characterization of thermomechanical and shape recovery properties, Polymer 54 (4) (2013) 1405–1414.
[20] M. Heuchel, T. Sauter, K. Kratz, A. Lendlein, Thermally induced shape-memory effects in polymers: quantification and related modeling approaches, J. Polym. Sci. Part B Polym. Phys. 51 (2013) 621–637, https://doi.org/10.1002/polb.23251.
[21] B. Xu, Y.Q. Fu, W.M. Huang, Y.T. Pei, Z.G. Chen, J.T.M. De Hosson, A. Kraft, R. L. Reuben, Thermal-mechanical properties of polyurethane-clay shape memory polymer nanocomposites, Polymers 2 (2010) 31–39, https://doi.org/10.3390/polym2020031.
[22] L. Domeier, A. Nissen, S. Goods, L. Whinnery, J. McElhanon, Thermomechanical characterization of thermoset urethane shape-memory polymer foams, J. Appl. Polym. Sci. 115 (6) (2009) 144–153, https://doi.org/10.1002/app.31413.
[23] P. Robinson, A. Bismark, B. Zhang, H.A. Maples, Deployable, shape memory carbon fibre composites without shape memory constituents, Compos. Sci. Technol. 145 (2017) 96–104, https://doi.org/10.1016/j.compscitech.2017.02.024.

[24] G.M. Tedde, L. Santo, D. Bellisario, L. Iorio, F. Quadrini, Frozen Stresses in shape memory polymer composites, Mater. Plast. 55 (2018) 494–497.
[25] Santo L., Iorio L., Tedde G.M., Quadrini F., 2018 "Shape memory behavior of carbon composites with functional interlayer", 13th International Manufacturing Science and Engineering Conference, MSEC 2018 2 Code 139921 (https://doi.org/10.1115/MSEC2018–6449).
[26] F. Quadrini, D. Bellisario, L. Iorio, L. Santo, Shape memory polymer composites by molding aeronautical prepregs with shape memory polymer interlayers, Mater. Res. Express 6 (11) (2019), https://doi.org/10.1088/2053-1591/ab50ad.
[27] F. Quadrini, L. Santo, E.A. Squeo, Shape memory epoxy foams for space applications, Materials Letters 69 (2012) 20–23, https://doi.org/10.1016/j.matlet.2011.11.050.
[28] F. Quadrini, E.A. Squeo, Solid-state foaming of epoxy resin, J. Cell. Plast. (2008) 44, https://doi.org/10.1177/0021955X07082486.
[29] L. Santo, F. Quadrini, P.L. Ganga, V. Zolesi, Mission BION-M1: results of RIBES/FOAM2 experiment on shape memory polymer foams and composites, Aerosp. Sci. Technol. 40 (2015) 109–114, https://doi.org/10.1016/j.ast.2014.11.008.
[30] F. Quadrini, D. Bellisario, L. Ciampoli, G. Costanza, L. Santo, Auxetic epoxy foams produced by solid state foaming, J. Cell. Plast. 52 (Issue 4) (2016) 441–454, https://doi.org/10.1177/0021955X15579456.
[31] F. Quadrini, Polymer matrix composites with shape memory properties, Mater. Sci. Forum 783–786 (2014) 2509–2516, http:// 10.4028/www.scientific.net/msf.783-786.2509.
[32] F. Quadrini, L. Iorio, D. Bellisario, L. Santo, Shape memory polymer composit unit with embedded heater, Smart Mater. Struct. 30 (7) (2021), 075009, https://doi.org/10.1088/1361-665X/ac00cb.
[33] L. Santo, F. Quadrini, E.A. Squeo, F. Dolce, G. Mascetti, D. Bertolotto, W. Villadei, P.L. Ganga, V. Zolesi, Behavior of shape memory epoxy foams in microgravity: experimental results of STS-134 mission, Microgravity Sci. Technol. 24 (2012) 287–296, https://doi.org/10.1007/s12217-012-9313-x.